

# Ab initio Materials Design of Superconductivity in $d^9$ Nickelates

Motoharu Kitatani,<sup>1,2</sup> Yusuke Nomura,<sup>3</sup> Motoaki Hirayama,<sup>1,4</sup> and Ryotaro Arita<sup>1,5</sup>

<sup>1</sup>RIKEN Center for Emergent Matter Science, 2-1 Hirosawa, Wako, Saitama 351-0198,

Japan

<sup>2</sup>Department of Material Science, University of Hyogo, Ako, Hyogo 678-1297, Japan

<sup>3</sup>Department of Applied Physics and Physico-Informatics, Keio University, 3-14-1 Hiyoshi, Kohoku-ku, Yokohama, 223-8522, Japan

<sup>4</sup>Quantum-Phase Electronics Center, The University of Tokyo, 7-3-1 Hongo, Bunkyo-ku, Tokyo 113-8656,

Japan

<sup>5</sup>Research Center for Advanced Science and Technology, University of Tokyo 4-6-1, Komaba, Meguro-ku, Tokyo 153-8904, Japan

(\*Electronic mail: kitatanimo@gmail.com)

(Dated: 3 May 2022)

Motivated by the recent theoretical materials design of superconducting  $d^9$  nickelates for which the charge transfer from the  $\text{NiO}_2$  to the block layer is completely suppressed [M. Hirayama *et al.*, Phys. Rev. B **101**, 075107 (2020)], we perform a calculation based on the dynamical vertex approximation and obtain the phase diagram of  $\text{RbCa}_2\text{NiO}_3$  and  $\text{A}_2\text{NiO}_2\text{Br}_2$  where A is a cation with a valence of 2.5+. We show that the phase diagram of these nickelates exhibits the same essential features as those found in cuprates. Namely, superconductivity appears upon hole-doping into an antiferromagnetic Mott insulator, and the superconducting transition temperature shows a dome-like shape. This demonstrates that the electron correlations play an essential role in nickelate superconductors and we can control them by changing block layers.

## I. INTRODUCTION

Unconventional superconductivity in strongly correlated electron systems such as the cuprates<sup>1</sup>, iron-based superconductors<sup>2</sup>,  $\text{Sr}_2\text{RuO}_4$ <sup>3</sup>, and  $\text{Na}_x\text{CoO}_2 \cdot y\text{H}_2\text{O}$ <sup>4</sup> has been one of the central issues in condensed matter physics. While we still lack a generally accepted explanation for their pairing mechanism, there is one characteristic common feature in these compounds: They have a crystal structure with stacked two-dimensional layers. For such layered materials, various families have been synthesized by inserting different layers or changing the stacking patterns.

It is of great interest to note that the recently discovered  $d^9$  nickelate superconductors<sup>5–11</sup>  $\text{RNiO}_2$  ( $R=\text{La, Pr, Nd}$ ) also share this common feature (for recent reviews, see, e.g., Refs. 12–20). Namely, they consist of the  $\text{NiO}_2$  layer and block layer, forming the infinite-layer structure. The maximum transition temperature  $T_c$  is about 15 K<sup>5–11</sup>. It is further enhanced to 20 ~ 30K by changing the substrate or applying pressure<sup>21–23</sup>. A theoretical phonon calculation has shown that the electron-phonon coupling is too weak to explain the experimental  $T_c$ <sup>24</sup>. Thus, the conventional mechanism is unlikely, and various unconventional mechanisms have been discussed theoretically<sup>25–38</sup>. On the experimental side, all the reports so far are consistent in that the pairing symmetry is not a simple  $s$ -wave, although there exists a discrepancy in the proposed symmetry<sup>39–41</sup>.

More recently, a quintuple-layer nickel superconductor  $\text{Nd}_6\text{Ni}_5\text{O}_{12}$  has been synthesized<sup>42</sup>. This has proven that superconductivity can be realized in nickelates other than infinite-layer compounds. Therefore, it is interesting to consider different layered structures and think of manipulating the electronic structure of nickelate superconductors. Indeed, a variety of theoretical materials design has been per-

formed<sup>43–45</sup>. In particular, it has been shown that we can control the charge transfer from the  $\text{NiO}_2$  layer to the block layer<sup>43</sup>.

In Fig. 1, we show the crystal structure, phonon dispersion, and electronic band dispersion of  $\text{NdNiO}_2$ <sup>17,24</sup>. We see that the electronic structure of  $\text{NdNiO}_2$  is similar to that of the cuprates in that only the  $3d_{x^2-y^2}$  orbital among the five  $3d$  orbitals contribute to the formation of the Fermi surface. The dispersion can be represented by a simple tight-binding model on the two-dimensional square lattice. However, there are also several distinct differences between  $\text{NdNiO}_2$  and the cuprates: In  $\text{NdNiO}_2$ , the oxygen  $2p$  level is far below the Fermi level, and the system belongs to the Mott-Hubbard regime<sup>46–48</sup> in the Zaanen-Sawatzky-Allen phase diagram<sup>49</sup>. Thus the hybridization between the oxygen  $2p$  and Ni  $3d$  orbitals is weaker than that in the cuprates which reside in the charge-transfer regime. In addition, there is substantial charge transfer from the  $\text{NiO}_2$  layer to the block layer<sup>50,51</sup>, and the Nd  $5d$  states and interstitial  $s$  state form Fermi pockets around the  $\Gamma$  and A points.

In Ref. 43, three of the present authors have shown that there are dynamically stable layered  $d^9$  nickelates for which the charge transfer from the  $\text{NiO}_2$  layer to the block layer is completely suppressed. There, only the Ni  $3d_{x^2-y^2}$  orbital forms a two-dimensional Fermi surface, whose shape is very similar to that of the cuprates. For these nickelates, effective low-energy models in terms of the Wannier functions<sup>52</sup> for the Ni  $3d_{x^2-y^2}$  orbital and O  $2p$  orbitals have been derived using the constrained random phase approximation (cRPA)<sup>53,54</sup>. In Ref. 55, the magnetic exchange coupling  $J$  in the  $\text{NiO}_2$  plane has also been estimated. While it has been known that the cuprate superconductors have a large exchange coupling of  $\sim 140$  meV<sup>56</sup>, these nickelates also have a significant exchange coupling as large as 80-100 meV<sup>57</sup>.

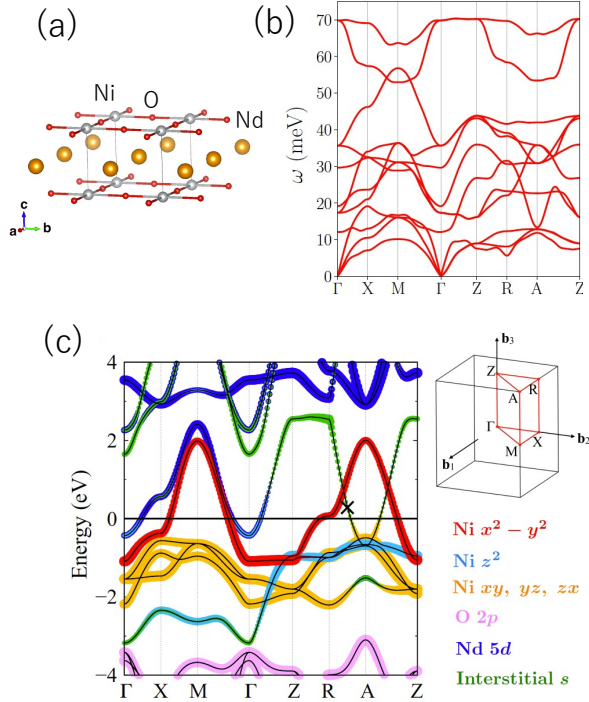


FIG. 1. (a) Crystal structure, (b) phonon dispersion, and (c) electronic structure of NdNiO<sub>2</sub>. Taken from Ref. 24 and Ref. 17.

In this paper, we extend these studies and calculate the phase diagram of RbCa<sub>2</sub>NiO<sub>3</sub> and A<sub>2</sub>NiO<sub>2</sub>Br<sub>2</sub> (A is a cation with a valence of 2.5+) by means of the dynamical vertex approximation (DΓA)<sup>58–60</sup>. The DΓA was also applied to study the phase diagram of the infinite-layer nickelate NdNiO<sub>2</sub><sup>31</sup> and quintuple-layer nickelate Nd<sub>6</sub>Ni<sub>5</sub>O<sub>12</sub><sup>61</sup>, which allows us to compare the phase diagram among nickelates. In RbCa<sub>2</sub>NiO<sub>3</sub> and A<sub>2</sub>NiO<sub>2</sub>Br<sub>2</sub>, differently from the infinite-layer nickelate NdNiO<sub>2</sub>, superconductivity emerges by a carrier doping into an antiferromagnetic insulator. The superconducting transition temperature ( $T_c$ ) shows a dome-like shape as a function of doping. Therefore, RbCa<sub>2</sub>NiO<sub>3</sub> and A<sub>2</sub>NiO<sub>2</sub>Br<sub>2</sub> may provide us with a unique opportunity to study the electron-hole asymmetry of the Mott insulating states in the nickelate superconductors.

The structure of the paper is as follows. In Section II, we discuss the phonon dispersion and electronic band dispersion of RbCa<sub>2</sub>NiO<sub>3</sub> and A<sub>2</sub>NiO<sub>2</sub>Br<sub>2</sub>. We show that these nickelates do not have imaginary phonon modes, indicating that they are dynamically stable. Thus although the crystal structures of these nickelates may not be the most stable structure, they are one of the meta-stable structures. Regarding the electronic structure, in contrast with the case of RNiO<sub>2</sub>, the charge transfer from the NiO<sub>2</sub> layer to the block layer in RbCa<sub>2</sub>NiO<sub>3</sub> and A<sub>2</sub>NiO<sub>2</sub>Br<sub>2</sub> is absent. In Section III, we show the results of *ab initio* derivation of the effective low-energy model (i.e., the single-orbital Hubbard model) for these nickelates. We see that RbCa<sub>2</sub>NiO<sub>3</sub> and A<sub>2</sub>NiO<sub>2</sub>Br<sub>2</sub> are more strongly correlated than NdNiO<sub>2</sub>. In Section IV, we solve the single-orbital Hub-

bard model derived in Section III using the DΓA. We obtain the phase diagram for RbCa<sub>2</sub>NiO<sub>3</sub> and A<sub>2</sub>NiO<sub>2</sub>Br<sub>2</sub> and compare it with that of NdNiO<sub>2</sub> and Nd<sub>6</sub>Ni<sub>5</sub>O<sub>12</sub>. In Section V, we summarize the results obtained in the present study.

## II. DYNAMICAL STABILITY AND ELECTRONIC STRUCTURE

Let us move on to the materials design of new nickelate superconductors<sup>43</sup>. Following the idea for the cuprate superconductors<sup>62</sup>, four types of block layers and six types of crystal structures for the nickelate superconductors have been proposed. The strategy to suppress the charge transfer from the NiO<sub>2</sub> layer to the block layer is the following: If we make the energy level of the block layer sufficiently higher than that of the Ni  $3d_{x^2-y^2}$  orbital, the charge transfer will not occur. Here, it should be noted that the level of Ni  $3d_{x^2-y^2}$  orbital is considerably higher than that of the Cu  $3d_{x^2-y^2}$  orbital in the cuprates. Thus, we should properly choose elements in the 1-3 groups (such as Sr and La) that strongly favor closed-shell electronic configuration. Following this strategy, the dynamical stability of 57 materials was examined in Ref. 43. While 16 compounds do not have imaginary phonon modes, we hereafter focus on RbCa<sub>2</sub>NiO<sub>3</sub> and A<sub>2</sub>NiO<sub>2</sub>Br<sub>2</sub> as representative compounds.

In Fig. 2 and Fig. 3, we show the crystal structure, phonon dispersion, and electronic structure of RbCa<sub>2</sub>NiO<sub>3</sub> and A<sub>2</sub>NiO<sub>2</sub>Br<sub>2</sub>, respectively. For the calculation of the phonon dispersion, the frozen-phonon method with a  $2 \times 2 \times 2$  or  $4 \times 4 \times 2$  supercell was employed. We see that calculation for the  $2 \times 2 \times 2$  supercell is enough to examine the presence/absence of imaginary modes. Since the calculation of the convex hull of ternary compounds is extremely expensive, we will not discuss whether these compounds are thermodynamically stable. However, from the results in Fig. 2(b) and Fig. 3(b), we can safely conclude that they are at least dynamically stable. Here, it is interesting to note that there is an experimental report of the synthesis of the  $d^8$  nickelate Sr<sub>2</sub>NiO<sub>2</sub>Cl<sub>2</sub><sup>63</sup>, which has the same crystal structure as A<sub>2</sub>NiO<sub>2</sub>Br<sub>2</sub>. The phonon band width is about 60-70 meV, which is similar to that of NdNiO<sub>2</sub> (see Fig. 1).

In Fig. 2(c) and Fig. 3(c), we show the electronic structure of RbCa<sub>2</sub>NiO<sub>3</sub> and A<sub>2</sub>NiO<sub>2</sub>Br<sub>2</sub>, respectively. Starting from these results, one can derive a single-orbital tight-binding model for the Ni  $3d_{x^2-y^2}$  orbital<sup>43</sup>. We highlight the band dispersion of the effective model with green dotted curves. As we discuss in Section III, the dispersion can be represented by a simple tight-binding model on the 2D square lattice. We also show the band minimum of the block-layer band with open circles. We see that the band minimum is higher than the Fermi level, so that the charge transfer from the NiO<sub>2</sub> to the block layer does not occur. Therefore, the effective Coulomb interaction between the Ni  $3d_{x^2-y^2}$  electrons tends to be stronger than that in RNiO<sub>2</sub> since the screening from the block layer becomes weaker.

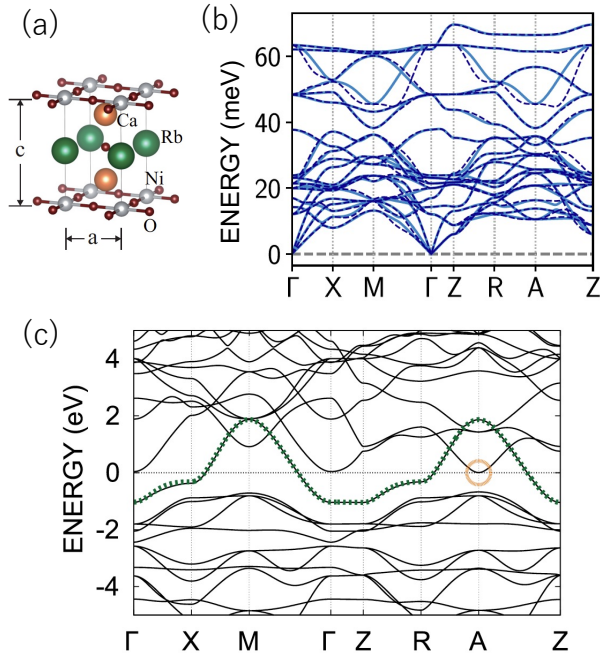


FIG. 2. (a) Crystal structure, (b) phonon dispersion, and (c) electronic structure of  $\text{RbCa}_2\text{NiO}_3$ . For the phonon calculation, the results for  $2 \times 2 \times 2$  and  $4 \times 4 \times 2$  supercells are shown with solid and dashed lines, respectively. The green dotted curves in (c) is the band dispersion of the single-orbital model. The open circle indicates the band minimum of the block-layer band. Taken from Ref. 43 and Ref. 55.

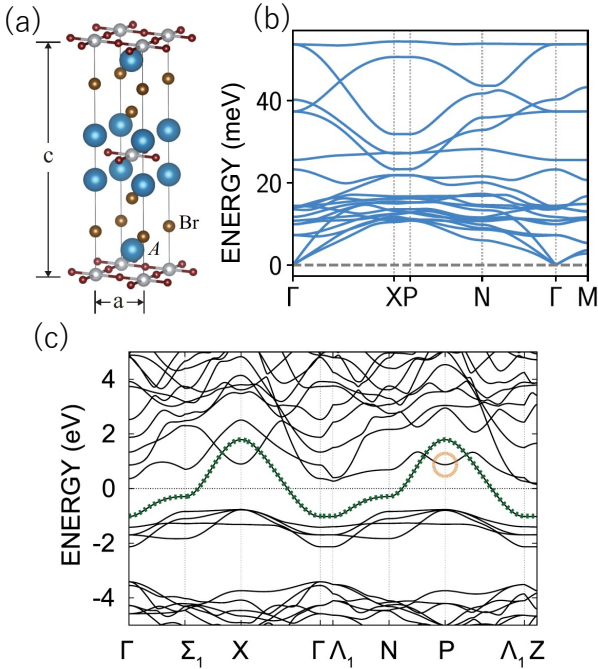


FIG. 3. (a) Crystal structure, (b) phonon dispersion, and (c) electronic structure of  $\text{A}_2\text{NiO}_2\text{Br}_2$  (A denotes a cation with a valence of  $2.5+$ ). For the phonon calculation, a  $2 \times 2 \times 2$  supercell was used. The green dotted curves in (c) is the band dispersion of the single-orbital model. The open circle indicates the band minimum of the block-layer band. Taken from Ref. 43 and Ref. 55.

TABLE I. Hopping and interaction parameters in the single-orbital Hubbard model.  $t$ ,  $t'$ ,  $t''$  are the nearest, next-nearest, and third-nearest hopping integrals, respectively.  $U$  is the onsite Hubbard interaction. The energy unit is eV. Taken from Ref. 24, Ref. 43 and Ref. 55.

	$t$	$t'$	$t''$	$U$	$ U/t $
$\text{NdNiO}_2$	-0.370	0.092	-0.045	2.608	7.052
$\text{RbCa}_2\text{NiO}_3$	-0.352	0.100	-0.046	3.347	9.522
$\text{A}_2\text{NiO}_2\text{Br}_2$	-0.337	0.089	-0.039	3.586	10.637

### III. EFFECTIVE LOW ENERGY MODELS

In this section, we look into the detail of the effective single-orbital model whose Hamiltonian is given by

$$\mathcal{H} = \sum_{ij\sigma} t_{ij} (c_{i\sigma}^\dagger c_{j\sigma} + h.c.) + U \sum_i n_{i\uparrow} n_{i\downarrow},$$

where  $c_{i\sigma}^\dagger$  and  $c_{i\sigma}$  are the creation and annihilation operator for the Ni  $3d_{x^2-y^2}$  orbital at site  $i$  with spin  $\sigma$ .  $n_{i\sigma} = c_{i\sigma}^\dagger c_{i\sigma}$  is the density operator. The transfer integrals  $\{t_{ij}\}$  between site  $i$  and  $j$  can be evaluated by calculating the matrix elements of the Kohn-Sham Hamiltonian ( $\mathcal{H}_{\text{KS}}$ ) in terms of the Wannier functions  $\{|\phi_{i\sigma}\rangle\}$  for the Ni  $3d_{x^2-y^2}$  orbital,

$$t_{ij} = \langle \phi_{i\sigma} | \mathcal{H}_{\text{KS}} | \phi_{j\sigma} \rangle.$$

On the other hand, the cRPA<sup>53</sup> is used to evaluate the effective Coulomb interaction in the model. It should be noted that the screening effect of the Ni  $3d_{x^2-y^2}$  electrons should be considered when we solve the effective model, and we should not take account of that effect when we derive the model. For this purpose, in the cRPA calculation, we first divide the polarization function  $P$  into the two parts,  $P_l$  and  $P_h$ . Here,  $P_l$  includes the contribution of the transition processes between the Ni  $3d_{x^2-y^2}$  states, and  $P_h$  is the other contributions to  $P$ . We then calculate

$$W_h = [1 - vP_h]^{-1}v,$$

where  $v$  is the bare Coulomb interaction. Since

$$W = [1 - vP]^{-1}v = [1 - W_h P_l]^{-1}W_h,$$

we see that  $W_h$  plays the role of the bare Coulomb interaction in the subspace of the Ni  $3d_{x^2-y^2}$  states. Taking the value of  $W_h$  in the limit of the zero frequency, the Hubbard  $U$  can be calculated as follows:

$$U = \langle \phi_{i\sigma} \phi_{i\sigma} | W_h(\omega = 0) | \phi_{i\sigma} \phi_{i\sigma} \rangle.$$

In Table I, we list the values of the transfer integrals between the nearest neighbor sites ( $t$ ), next nearest neighbor sites ( $t'$ ), third nearest neighbor sites ( $t''$ ), and Hubbard  $U$ <sup>24,43,55</sup>. We see that the ratio between  $U$  and  $t$  in  $\text{RbCa}_2\text{NiO}_3$  and  $\text{A}_2\text{NiO}_2\text{Br}_2$  is substantially larger than that in  $\text{NdNiO}_2$ .

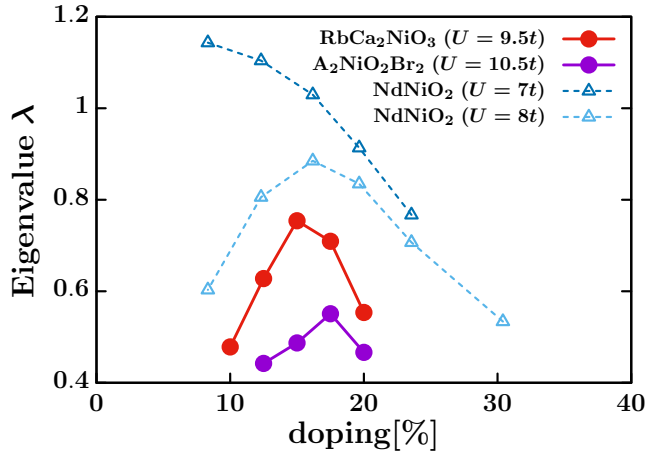


FIG. 4. Leading superconductivity eigenvalues for NdNiO<sub>2</sub>, RbCa<sub>2</sub>NiO<sub>3</sub>, and A<sub>2</sub>NiO<sub>2</sub>Br<sub>2</sub> at fixed temperature  $T = 0.01t$ . NdNiO<sub>2</sub> results are taken from Ref.31.

#### IV. DΓA CALCULATION AND PHASE DIAGRAM

Next, let's analyze the correlation effect of these effective low energy models for studying the superconductivity property. Based on Table I, we studied the two dimensional Hubbard model with hoppings:  $t'/t = -0.28$ ,  $t''/t = 0.13$ ,  $U = 9.5t$  for RbCa<sub>2</sub>NiO<sub>3</sub> and  $t'/t = -0.26$ ,  $t''/t = 0.12$ ,  $U = 10.5t$  for A<sub>2</sub>NiO<sub>2</sub>Br<sub>2</sub>. Here, we employ the DΓA<sup>58–60</sup>, which is one of the diagrammatic extensions of the dynamical mean field theory (DMFT)<sup>64–66</sup>. The DΓA can capture the strongly correlated effect and the long-range fluctuation effect beyond DMFT, both of which are essential for describing the layered unconventional superconductivity with strong correlations. The method has succeeded in describing the phase diagram of the unconventional superconductivity<sup>31,67</sup>, e.g., cuprates and nickelates. In calculation details, we follow the previous paper about the infinite layer nickelates<sup>31</sup>. Please see that paper or review articles<sup>60,68,69</sup> for more information about the method.

In Fig. 4, we show the DΓA result of leading eigenvalues of the linearized gap function in the  $d$ -wave (singlet, even-frequency) channel against the hole doping level. Here, we also show NdNiO<sub>2</sub> results taken from Ref. 31, where the charge transfer effect is also taken into account. The eigenvalue is often used as the measure of  $T_c$  since it usually monotonically increases as decreasing the temperature and the phase transition occurs when the eigenvalue reaches the unity. We can see that both RbCa<sub>2</sub>NiO<sub>3</sub> and A<sub>2</sub>NiO<sub>2</sub>Br<sub>2</sub> show the dome structure of the superconductivity instability peaked at around 15-20% doping like cuprates and the infinite-layer nickelates. On the other hand, eigenvalues are lower than the infinite-layer system<sup>31</sup> or the quintuple-layer system<sup>61</sup>. Some theoretical studies suggest that the infinite-layer nickelate material resides in the strong-coupling regime of superconductivity<sup>25,31</sup>. Indeed, the  $T_c$  change in recent pressure and strain experiments<sup>21–23</sup> can be reasonably understood by the change of the effective interaction strength. Both materials consid-

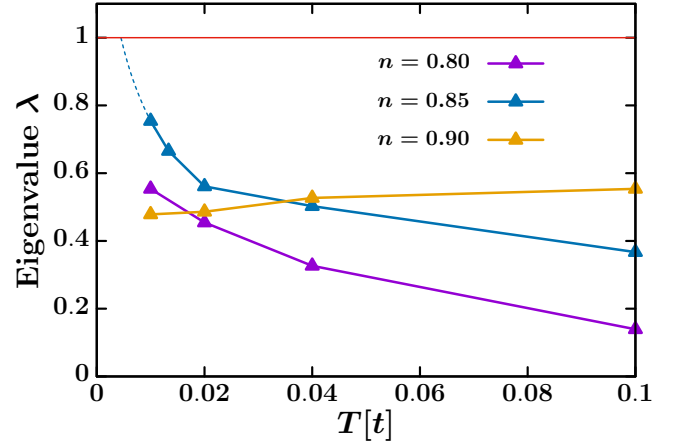


FIG. 5. Temperature dependence of the superconductivity eigenvalue for RbCa<sub>2</sub>NiO<sub>3</sub>.

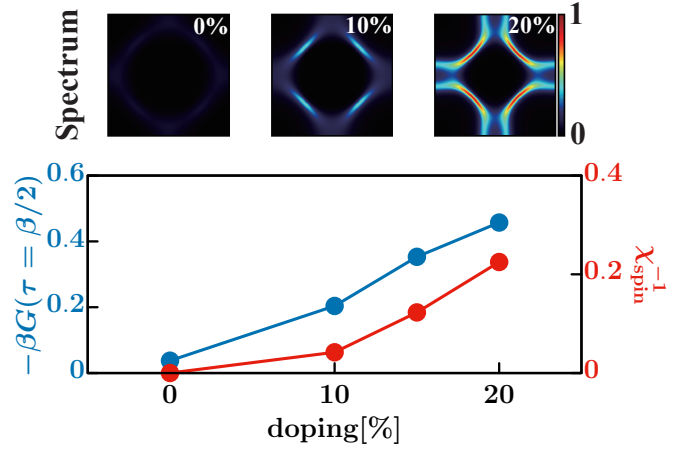


FIG. 6. Filling dependence of the spectrum (Green function) and the spin susceptibility  $\chi_{\text{spin}}(\mathbf{Q}_{\text{max}}, \omega = 0)$  for RbCa<sub>2</sub>NiO<sub>3</sub> ( $t'/t = -0.28$ ,  $t''/t = 0.13$ ) at  $T = 0.04t$ .

ered here have further large  $U/t$  values, and then we obtained weaker superconductivity instability.

We also show the temperature dependence of eigenvalues for RbCa<sub>2</sub>NiO<sub>3</sub> in Fig. 5. At the optimal doping regime at  $n = 0.85$ , we obtained the transition temperature  $T_c \sim 0.0045t \sim 18$  K by extrapolating the DΓA result with the fit function  $\lambda(T) = a - b \ln(T)$ <sup>31,70</sup>. Here we just used the  $U/t$  value obtained from cRPA calculations. If we employ a somewhat larger  $U/t$  value like Ref. 31,  $T_c$  will further decrease.

Furthermore, we show the filling dependence of the spectrum and spin fluctuation in Fig. 6. As a proxy of the spectrum, we here show the momentum dependence of the imaginary part of the Green function at the lowest Matsubara frequency  $-\frac{1}{\pi}G(\mathbf{k}, \omega_n = \pi/\beta)$  and the momentum averaged Green function at  $\tau = \beta/2$ . Without doping, we can see the similarity with cuprates: the spectral weight at the Fermi level is strongly suppressed by the self-energy, and spin fluctuation becomes strongly enhanced so that antiferromagnetism will stabilize once we consider the weak three dimensionality.

## V. CONCLUSION

In conclusion, we performed a calculation based on the dynamical vertex approximation and obtain the phase diagram of  $\text{RbCa}_2\text{NiO}_3$  and  $\text{A}_2\text{NiO}_2\text{Br}_2$ . In these materials, the charge transfer from the  $\text{NiO}_2$  layer to the block layer is absent, and the effective Coulomb interaction between  $\text{Ni } 3d_{x^2-y^2}$  electrons is stronger than that in  $\text{RNiO}_2$  or  $\text{Nd}_6\text{Ni}_5\text{O}_{12}$ . We obtained the dome shaped superconductivity instability like infinite layer nickelates. While the estimated  $T_c$  is lower than  $\text{RNiO}_2$ <sup>31</sup>, we here demonstrate that we can control the charge transfer and correlation effect among nickelate compounds by changing block layers. Furthermore,  $\text{RbCa}_2\text{NiO}_3$  and  $\text{A}_2\text{NiO}_2\text{Br}_2$  may provide us with a unique opportunity to study the electron-hole asymmetry of the Mott insulating states in the nickelate superconductors.

## ACKNOWLEDGMENTS

We are grateful for fruitful discussions with Karsten Held, Liang Si, Paul Worm, Terumasa Tadano, Takuya Nomoto, and Kazuma Nakamura. We acknowledge the financial support by Grant-in-Aids for Scientific Research (JSPS KAKENHI) [Grant No. JP20K22342 (MK), JP21K13887 (MK), JP20K14423 (YN), JP21H01041 (YN), and JP19H05825 (RA)] and MEXT as “Program for Promoting Researches on the Supercomputer Fugaku” (Basic Science for Emergence and Functionality in Quantum Matter—Innovative Strongly-Correlated Electron Science by Integration of “Fugaku” and Frontier Experiments—) (JPMXP1020200104). A part of the calculation has been done on MASAMUNE-IMR of the Center for Computational Materials Science, Tohoku University.

## DATA AVAILABILITY STATEMENT

The data that support the findings of this study are available within the article.

- <sup>1</sup>J. G. Bednorz and K. A. Müller, “Possible high  $T_c$  superconductivity in the Ba-La-Cu-O system,” *Zeitschrift für Physik B Condensed Matter* **64**, 189–193 (1986).
- <sup>2</sup>Y. Kamihara, T. Watanabe, M. Hirano, and H. Hosono, “Iron-Based Layered Superconductor  $\text{La}[\text{O}_{1-x}\text{F}_x]\text{FeAs}$  ( $x = 0.05\text{--}0.12$ ) with  $T_c = 26$  K,” *Journal of the American Chemical Society* **130**, 3296–3297 (2008).
- <sup>3</sup>Y. Maeno, H. Hashimoto, K. Yoshida, S. Nishizaki, T. Fujita, J. G. Bednorz, and F. Lichtenberg, “Superconductivity in a layered perovskite without copper,” *Nature* **372**, 532–534 (1994).
- <sup>4</sup>K. Takada, H. Sakurai, E. Takayama-Muromachi, F. Izumi, R. A. Dilanian, and T. Sasaki, “Superconductivity in two-dimensional  $\text{CoO}_2$  layers,” *Nature* **422**, 53–55 (2003).
- <sup>5</sup>D. Li, K. Lee, B. Y. Wang, M. Osada, S. Crossley, H. R. Lee, Y. Cui, Y. Hikita, and H. Y. Hwang, “Superconductivity in an infinite-layer nickelate,” *Nature* **572**, 624–627 (2019).
- <sup>6</sup>D. Li, B. Y. Wang, K. Lee, S. P. Harvey, M. Osada, B. H. Goodge, L. F. Kourkoutis, and H. Y. Hwang, “Superconducting Dome in  $\text{Nd}_{1-x}\text{Sr}_x\text{NiO}_2$  Infinite Layer Films,” *Phys. Rev. Lett.* **125**, 027001 (2020).
- <sup>7</sup>M. Osada, B. Y. Wang, B. H. Goodge, K. Lee, H. Yoon, K. Sakuma, D. Li, M. Miura, L. F. Kourkoutis, and H. Y. Hwang, “A Superconducting Praseodymium Nickelate with Infinite Layer Structure,” *Nano Letters* **20**, 5735–5740 (2020).
- <sup>8</sup>M. Osada, B. Y. Wang, K. Lee, D. Li, and H. Y. Hwang, “Phase diagram of infinite layer praseodymium nickelate  $\text{Pr}_{1-x}\text{Sr}_x\text{NiO}_2$  thin films,” *Phys. Rev. Materials* **4**, 121801 (2020).
- <sup>9</sup>M. Osada, B. Y. Wang, B. H. Goodge, S. P. Harvey, K. Lee, D. Li, L. F. Kourkoutis, and H. Y. Hwang, “Nickelate Superconductivity without Rare-Earth Magnetism:  $(\text{La},\text{Sr})\text{NiO}_2$ ,” *Advanced Materials* **33**, 2104083 (2021).
- <sup>10</sup>S. Zeng, C. S. Tang, X. Yin, C. Li, M. Li, Z. Huang, J. Hu, W. Liu, G. J. Omar, H. Jani, Z. S. Lim, K. Han, D. Wan, P. Yang, S. J. Pennycook, A. T. S. Wee, and A. Ariando, “Phase Diagram and Superconducting Dome of Infinite-Layer  $\text{Nd}_{1-x}\text{Sr}_x\text{NiO}_2$  Thin Films,” *Phys. Rev. Lett.* **125**, 147003 (2020).
- <sup>11</sup>S. Zeng, C. Li, L. E. Chow, Y. Cao, Z. Zhang, C. S. Tang, X. Yin, Z. S. Lim, J. Hu, P. Yang, and A. Ariando, “Superconductivity in infinite-layer nickelate  $\text{La}_{1-x}\text{Ca}_x\text{NiO}_2$  thin films,” *Sci. Adv.* **8**, eabl9927 (2022).
- <sup>12</sup>M. R. Norman, “Entering the Nickel Age of Superconductivity,” *Physics* **13**, 85 (2020).
- <sup>13</sup>W. E. Pickett, “The dawn of the nickel age of superconductivity,” *Nature Reviews Physics* **3**, 7–8 (2021).
- <sup>14</sup>J. Zhang and X. Tao, “Review on quasi-2D square planar nickelates,” *CrysEngComm* **23**, 3249–3264 (2021).
- <sup>15</sup>A. S. Botana, F. Bernardini, and A. Cano, “Nickelate Superconductors: An Ongoing Dialog between Theory and Experiments,” *Journal of Experimental and Theoretical Physics* **132**, 618–627 (2021).
- <sup>16</sup>Y. Ji, J. Liu, L. Li, and Z. Liao, “Superconductivity in infinite layer nickelates,” *Journal of Applied Physics* **130**, 060901 (2021).
- <sup>17</sup>Y. Nomura and R. Arita, “Superconductivity in infinite-layer nickelates,” *Reports on Progress in Physics* **85**, 052501 (2022).
- <sup>18</sup>Q. Gu and H.-H. Wen, “Superconductivity in nickel-based 112 systems,” *The Innovation* **3**, 100202 (2022).
- <sup>19</sup>L. E. Chow and A. Ariando, “Infinite-Layer Nickelate Superconductors: A Current Experimental Perspective of the Crystal and Electronic Structures,” *Frontiers in Physics* **10** (2022).
- <sup>20</sup>X. Zhou, P. Qin, Z. Feng, H. Yan, X. Wang, H. Chen, Z. Meng, and Z. Liu, “Experimental progress on the emergent infinite-layer Ni-based superconductors,” *Materials Today* (2022).
- <sup>21</sup>X. Ren, Q. Gao, Y. Zhao, H. Luo, X. Zhou, and Z. Zhu, “Superconductivity in infinite-layer  $\text{Pr}_{0.8}\text{Sr}_{0.2}\text{NiO}_2$  films on different substrates,” *arXiv preprint arXiv:2109.05761* (2021).
- <sup>22</sup>N. Wang, M. Yang, K. Chen, Z. Yang, H. Zhang, Z. Zhu, Y. Uwatoko, X. Dong, K. Jin, J. Sun, *et al.*, “Pressure-induced monotonic enhancement of  $T_c$  to over 30 K in the superconducting  $\text{Pr}_{0.82}\text{Sr}_{0.18}\text{NiO}_2$  thin films,” *arXiv preprint arXiv:2109.12811* (2021).
- <sup>23</sup>K. Lee, B. Y. Wang, M. Osada, B. H. Goodge, T. C. Wang, Y. Lee, S. Harvey, W. J. Kim, Y. Yu, C. Murthy, *et al.*, “Character of the “normal state” of the nickelate superconductors,” *arXiv preprint arXiv:2203.02580* (2022).
- <sup>24</sup>Y. Nomura, M. Hirayama, T. Tadano, Y. Yoshimoto, K. Nakamura, and R. Arita, “Formation of a two-dimensional single-component correlated electron system and band engineering in the nickelate superconductor  $\text{NdNiO}_2$ ,” *Phys. Rev. B* **100**, 205138 (2019).
- <sup>25</sup>H. Sakakibara, H. Usui, K. Suzuki, T. Kotani, H. Aoki, and K. Kuroki, “Model Construction and a Possibility of Cupratelike Pairing in a New  $d^9$  Nickelate Superconductor  $(\text{Nd},\text{Sr})\text{NiO}_2$ ,” *Phys. Rev. Lett.* **125**, 077003 (2020).
- <sup>26</sup>J. Hirsch and F. Marsiglio, “Hole superconductivity in infinite-layer nickelates,” *Physica C: Superconductivity and its Applications* **566**, 1353534 (2019).
- <sup>27</sup>X. Wu, D. Di Sante, T. Schwemmer, W. Hanke, H. Y. Hwang, S. Raghu, and R. Thomale, “Robust  $d_{x^2-y^2}$ -wave superconductivity of infinite-layer nickelates,” *Phys. Rev. B* **101**, 060504 (2020).
- <sup>28</sup>P. Werner and S. Hoshino, “Nickelate superconductors: Multiorbital nature and spin freezing,” *Phys. Rev. B* **101**, 041104 (2020).
- <sup>29</sup>Y.-H. Zhang and A. Vishwanath, “Type-II  $t$ - $J$  model in superconducting nickelate  $\text{Nd}_{1-x}\text{Sr}_x\text{NiO}_2$ ,” *Phys. Rev. Research* **2**, 023112 (2020).
- <sup>30</sup>J. Chang, J. Zhao, and Y. Ding, “Hund-Heisenberg model in superconducting infinite-layer nickelates,” *The European Physical Journal B* **93**, 220 (2020).
- <sup>31</sup>M. Kitatani, L. Si, O. Janson, R. Arita, Z. Zhong, and K. Held, “Nickelate superconductors—a renaissance of the one-band Hubbard model,” *npj Quantum Materials* **5**, 59 (2020).



- <sup>32</sup>P. Adhikary, S. Bandyopadhyay, T. Das, I. Dasgupta, and T. Saha-Dasgupta, “Orbital-selective superconductivity in a two-band model of infinite-layer nickelates,” *Phys. Rev. B* **102**, 100501 (2020).
- <sup>33</sup>Z. Wang, G.-M. Zhang, Y.-f. Yang, and F.-C. Zhang, “Distinct pairing symmetries of superconductivity in infinite-layer nickelates,” *Phys. Rev. B* **102**, 220501 (2020).
- <sup>34</sup>C. Lu, L.-H. Hu, Y. Wang, F. Yang, and C. Wu, “Two-orbital model for possible superconductivity pairing mechanism in nickelates,” *Phys. Rev. B* **105**, 054516 (2022).
- <sup>35</sup>T. Y. Xie, Z. Liu, C. Cao, Z. F. Wang, J. L. Yang, and W. Zhu, “Microscopic Theory of Superconducting Phase Diagram in Infinite-Layer Nickelates,” (2021), arXiv:2112.01677 [cond-mat.str-el].
- <sup>36</sup>J. Karp, A. Hampel, and A. J. Millis, “Superconductivity and Antiferromagnetism in NdNiO<sub>2</sub> and CaCuO<sub>2</sub>: A Cluster DMFT Study,” (2022), arXiv:2201.10481 [cond-mat.str-el].
- <sup>37</sup>M. Jiang, “Characterizing the superconducting instability in a two-orbital  $d$ - $s$  model: insights to infinite-layer nickelate superconductors,” (2022), arXiv:2201.12967 [cond-mat.supr-con].
- <sup>38</sup>A. Kreisel, B. M. Andersen, A. T. Rømer, I. M. Eremin, and F. Lechermann, “Superconducting Instabilities in Strongly-Correlated Infinite-Layer Nickelates,” (2022), arXiv:2202.11135 [cond-mat.supr-con].
- <sup>39</sup>Q. Gu, Y. Li, S. Wan, H. Li, W. Guo, H. Yang, Q. Li, X. Zhu, X. Pan, Y. Nie, and H.-H. Wen, “Single particle tunneling spectrum of superconducting Nd<sub>1-x</sub>Sr<sub>x</sub>NiO<sub>2</sub> thin films,” *Nat. Commun.* **11**, 6027 (2020).
- <sup>40</sup>L. E. Chow, S. K. Sudheesh, P. Nandi, S. W. Zeng, Z. T. Zhang, X. M. Du, Z. S. Lim, E. E. M. Chia, and A. Ariando, “Pairing symmetry in infinite-layer nickelate superconductor,” (2022), arXiv:2201.10038 [cond-mat.supr-con].
- <sup>41</sup>S. P. Harvey, B. Y. Wang, J. Fowlie, M. Osada, K. Lee, Y. Lee, D. Li, and H. Y. Hwang, “Evidence for nodal superconductivity in infinite-layer nickelates,” (2022), arXiv:2201.12971 [cond-mat.supr-con].
- <sup>42</sup>G. A. Pan, D. Ferenc Segedin, H. LaBollita, Q. Song, E. M. Nica, B. H. Goodge, A. T. Pierce, S. Doyle, S. Novakov, D. Córdoba Carrizales, A. T. N’Diaye, P. Shafer, H. Paik, J. T. Heron, J. A. Mason, A. Yacoby, L. F. Kourkoutis, O. Erten, C. M. Brooks, A. S. Botana, and J. A. Mundy, “Superconductivity in a quintuple-layer square-planar nickelate,” *Nature Materials* (2021).
- <sup>43</sup>M. Hirayama, T. Tadano, Y. Nomura, and R. Arita, “Materials design of dynamically stable  $d^9$  layered nickelates,” *Phys. Rev. B* **101**, 075107 (2020).
- <sup>44</sup>N. Kitamine, M. Ochi, and K. Kuroki, “Designing nickelate superconductors with  $d^8$  configuration exploiting mixed-anion strategy,” *Phys. Rev. Research* **2**, 042032 (2020).
- <sup>45</sup>M.-C. Jung, H. LaBollita, V. Pardo, and A. S. Botana, “Antiferromagnetic insulating state in layered nickelates at half-filling,” (2022), arXiv:2012.02711 [cond-mat.supr-con].
- <sup>46</sup>M. Hepting, D. Li, C. J. Jia, H. Lu, E. Paris, Y. Tseng, X. Feng, M. Osada, E. Been, Y. Hikita, Y. D. Chuang, Z. Hussain, K. J. Zhou, A. Nag, M. Garcia-Fernandez, M. Rossi, H. Y. Huang, D. J. Huang, Z. X. Shen, T. Schmitt, H. Y. Hwang, B. Moritz, J. Zaanen, T. P. Devereaux, and W. S. Lee, “Electronic structure of the parent compound of superconducting infinite-layer nickelates,” *Nature Materials* **19**, 381–385 (2020).
- <sup>47</sup>Y. Fu, L. Wang, H. Cheng, S. Pei, X. Zhou, J. Chen, S. Wang, R. Zhao, W. Jiang, C. Liu, M. Huang, X. Wang, Y. Zhao, D. Yu, F. Ye, S. Wang, and J.-W. Mei, “Core-level x-ray photoemission and Raman spectroscopy studies on electronic structures in Mott-Hubbard type nickelate oxide NdNiO<sub>2</sub>,” (2019), arXiv:arXiv:1911.03177 [cond-mat.supr-con].
- <sup>48</sup>B. H. Goodge, D. Li, K. Lee, M. Osada, B. Y. Wang, G. A. Sawatzky, H. Y. Hwang, and L. F. Kourkoutis, “Doping evolution of the Mott-Hubbard landscape in infinite-layer nickelates,” *Proceedings of the National Academy of Sciences* **118** (2021).
- <sup>49</sup>J. Zaanen, G. A. Sawatzky, and J. W. Allen, “Band gaps and electronic structure of transition-metal compounds,” *Phys. Rev. Lett.* **55**, 418–421 (1985).
- <sup>50</sup>K.-W. Lee and W. E. Pickett, “Infinite-layer LaNiO<sub>2</sub>: Ni<sup>1+</sup> is not Cu<sup>2+</sup>,” *Phys. Rev. B* **70**, 165109 (2004).
- <sup>51</sup>A. S. Botana and M. R. Norman, “Similarities and Differences between LaNiO<sub>2</sub> and CaCuO<sub>2</sub> and Implications for Superconductivity,” *Phys. Rev. X* **10**, 011024 (2020).
- <sup>52</sup>G. Pizzi, V. Vitale, R. Arita, S. Blügel, F. Freimuth, G. G. eranton, M. Gibertini, D. Gresch, C. Johnson, T. Koretsune, J. Ibañez-Azpiroz, H. Lee, J.-M. Lihm, D. Marchand, A. Marrazzo, Y. Mokrousov, J. I. Mustafa, Y. No-hara, Y. Nomura, L. Paulatto, S. Ponc̃e, T. Ponweiser, J. Qiao, F. Thöle, S. S. Tsirkin, M. Wierzbowska, N. Marzari, D. Vanderbilt, I. Souza, A. A. Mostofi, and J. R. Yates, “Wannier90 as a community code: new features and applications,” *Journal of Physics: Condensed Matter* **32**, 165902 (2020).
- <sup>53</sup>F. Aryasetiawan, M. Imada, A. Georges, G. Kotliar, S. Biermann, and A. I. Lichtenstein, “Frequency-dependent local interactions and low-energy effective models from electronic structure calculations,” *Phys. Rev. B* **70**, 195104 (2004).
- <sup>54</sup>K. Nakamura, Y. Yoshimoto, Y. Nomura, T. Tadano, M. Kawamura, T. Kotsugi, K. Yoshimi, T. Misawa, and Y. Motoyama, “Respack: An ab initio tool for derivation of effective low-energy model of material,” *Computer Physics Communications* **261**, 107781 (2021).
- <sup>55</sup>Y. Nomura, T. Nomoto, M. Hirayama, and R. Arita, “Magnetic exchange coupling in cuprate-analog  $d^9$  nickelates,” *Phys. Rev. Research* **2**, 043144 (2020).
- <sup>56</sup>P. A. Lee, N. Nagaosa, and X.-G. Wen, “Doping a mott insulator: Physics of high-temperature superconductivity,” *Rev. Mod. Phys.* **78**, 17–85 (2006).
- <sup>57</sup>We note that the strength of the magnetic exchange coupling  $J$  in the infinite-layer nickelates is controversial. Experimentally, Ref. 47 (Raman experiment using NdNiO<sub>2</sub> bulk samples) and Ref. 71 (resonant inelastic X-ray scattering experiment for NdNiO<sub>2</sub> thin film samples) gave  $J = 25$  meV and  $J = 64(3)$  meV, respectively. There is no agreement in the theoretical estimates, either<sup>72–83</sup>. Because the infinite-layer nickelates are not a Mott insulator, an ambiguity exists in the mapping to spin models, which is one of the reasons for the discrepancy in the theoretical estimates<sup>55</sup>.
- <sup>58</sup>A. Toschi, A. A. Katanin, and K. Held, “Dynamical vertex approximation: A step beyond dynamical mean-field theory,” *Phys. Rev. B* **75**, 045118 (2007).
- <sup>59</sup>A. A. Katanin, A. Toschi, and K. Held, “Comparing pertinent effects of antiferromagnetic fluctuations in the two- and three-dimensional hubbard model,” *Phys. Rev. B* **80**, 075104 (2009).
- <sup>60</sup>G. Rohringer, H. Hafermann, A. Toschi, A. A. Katanin, A. E. Antipov, M. I. Katsnelson, A. I. Lichtenstein, A. N. Rubtsov, and K. Held, “Diagrammatic routes to nonlocal correlations beyond dynamical mean field theory,” *Rev. Mod. Phys.* **90**, 025003 (2018).
- <sup>61</sup>P. Worm, L. Si, M. Kitatani, R. Arita, J. M. Tomczak, and K. Held, “Correlations turn electronic structure of finite-layer nickelates upside down,” (2021), arXiv:2111.12697 [cond-mat.supr-con].
- <sup>62</sup>Y. Tokura and T. Arima, “New classification method for layered copper oxide compounds and its application to design of new high T<sub>c</sub> superconductors,” *Jpn. J. Appl. Phys.* **29**, 2388–2402 (1990).
- <sup>63</sup>Y. Tsujimoto, C. I. Sathish, Y. Matsushita, K. Yamaura, and T. Uchikoshi, “New members of layered oxychloride perovskites with square planar coordination: Sr<sub>2</sub>MO<sub>2</sub>Cl<sub>2</sub> ( $M = \text{Mn, Ni}$ ) and Ba<sub>2</sub>PdO<sub>2</sub>Cl<sub>2</sub>,” *Chem. Commun.* **50**, 5915–5918 (2014).
- <sup>64</sup>W. Metzner and D. Vollhardt, “Correlated lattice fermions in  $d = \infty$  dimensions,” *Phys. Rev. Lett.* **62**, 324–327 (1989).
- <sup>65</sup>A. Georges and G. Kotliar, “Hubbard model in infinite dimensions,” *Phys. Rev. B* **45**, 6479–6483 (1992).
- <sup>66</sup>A. Georges, G. Kotliar, W. Krauth, and M. J. Rozenberg, “Dynamical mean-field theory of strongly correlated fermion systems and the limit of infinite dimensions,” *Rev. Mod. Phys.* **68**, 13–125 (1996).
- <sup>67</sup>M. Kitatani, T. Schäfer, H. Aoki, and K. Held, “Why the critical temperature of high- $T_c$  cuprate superconductors is so low: The importance of the dynamical vertex structure,” *Phys. Rev. B* **99**, 041115 (2019).
- <sup>68</sup>K. Held, L. Si, P. Worm, O. Janson, R. Arita, Z. Zhong, J. M. Tomczak, and M. Kitatani, “Phase diagram of nickelate superconductors calculated by dynamical vertex approximation,” *Frontiers in Physics* **9** (2022), 10.3389/fphy.2021.810394.
- <sup>69</sup>M. Kitatani, R. Arita, T. Schäfer, and K. Held, “Strongly correlated superconductivity with long-range spatial fluctuations,” arXiv preprint arXiv:2203.12844 (2022).
- <sup>70</sup>A. Sekine, J. Nasu, and S. Ishihara, “Polar charge fluctuation and superconductivity in organic conductors,” *Phys. Rev. B* **87**, 085133 (2013).
- <sup>71</sup>H. Lu, M. Rossi, A. Nag, M. Osada, D. F. Li, K. Lee, B. Y. Wang, M. Garcia-Fernandez, S. Agrestini, Z. X. Shen, E. M. Been, B. Moritz, T. P. Devereaux, J. Zaanen, H. Y. Hwang, K.-J. Zhou, and W. S. Lee, “Magnetic excitations in infinite-layer nickelates,” *Science* **373**, 213–216 (2021).

- <sup>72</sup>M. Jiang, M. Berciu, and G. A. Sawatzky, “Critical Nature of the Ni Spin State in Doped NdNiO<sub>2</sub>,” *Phys. Rev. Lett.* **124**, 207004 (2020).
- <sup>73</sup>S. Ryee, H. Yoon, T. J. Kim, M. Y. Jeong, and M. J. Han, “Induced magnetic two-dimensionality by hole doping in the superconducting infinite-layer nickelate Nd<sub>1-x</sub>Sr<sub>x</sub>NiO<sub>2</sub>,” *Phys. Rev. B* **101**, 064513 (2020).
- <sup>74</sup>H. Zhang, L. Jin, S. Wang, B. Xi, X. Shi, F. Ye, and J.-W. Mei, “Effective Hamiltonian for nickelate oxides Nd<sub>1-x</sub>Sr<sub>x</sub>NiO<sub>2</sub>,” *Phys. Rev. Research* **2**, 013214 (2020).
- <sup>75</sup>G.-M. Zhang, Y.-F. Yang, and F.-C. Zhang, “Self-doped Mott insulator for parent compounds of nickelate superconductors,” *Phys. Rev. B* **101**, 020501 (2020).
- <sup>76</sup>Z. Liu, Z. Ren, W. Zhu, Z. Wang, and J. Yang, “Electronic and magnetic structure of infinite-layer NdNiO<sub>2</sub>: trace of antiferromagnetic metal,” *npj Quantum Materials* **5**, 31 (2020).
- <sup>77</sup>E. Been, W.-S. Lee, H. Y. Hwang, Y. Cui, J. Zaanen, T. Devereaux, B. Moritz, and C. Jia, “Electronic Structure Trends Across the Rare-Earth Series in Superconducting Infinite-Layer Nickelates,” *Phys. Rev. X* **11**, 011050 (2021).
- <sup>78</sup>I. Leonov, S. L. Skornyakov, and S. Y. Savrasov, “Lifshitz transition and frustration of magnetic moments in infinite-layer NdNiO<sub>2</sub> upon hole doping,” *Phys. Rev. B* **101**, 241108 (2020).
- <sup>79</sup>I. Leonov, “Effect of lattice strain on the electronic structure and magnetic correlations in infinite-layer (Nd,Sr)NiO<sub>2</sub>,” *Journal of Alloys and Compounds* **883**, 160888 (2021).
- <sup>80</sup>X. Wan, V. Ivanov, G. Resta, I. Leonov, and S. Y. Savrasov, “Exchange interactions and sensitivity of the Ni two-hole spin state to Hund’s coupling in doped NdNiO<sub>2</sub>,” *Phys. Rev. B* **103**, 075123 (2021).
- <sup>81</sup>Z.-J. Lang, R. Jiang, and W. Ku, “Strongly correlated doped hole carriers in the superconducting nickelates: Their location, local many-body state, and low-energy effective Hamiltonian,” *Phys. Rev. B* **103**, L180502 (2021).
- <sup>82</sup>V. M. Katukuri, N. A. Bogdanov, O. Weser, J. van den Brink, and A. Alavi, “Electronic correlations and magnetic interactions in infinite-layer NdNiO<sub>2</sub>,” *Phys. Rev. B* **102**, 241112 (2020).
- <sup>83</sup>R. Zhang, C. Lane, B. Singh, J. Nokelainen, B. Barbiellini, R. S. Markiewicz, A. Bansil, and J. Sun, “Magnetic and *f*-electron effects in LaNiO<sub>2</sub> and NdNiO<sub>2</sub> nickelates with cuprate-like  $3d_{x^2-y^2}$  band,” *Communications Physics* **4**, 118 (2021).